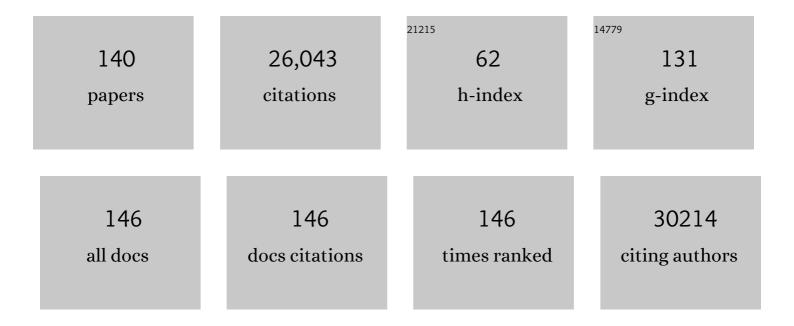
Yiying Wu

List of Publications by Year in descending order

Source: https://exaly.com/author-pdf/2088094/publications.pdf Version: 2024-02-01



#	Article	IF	CITATIONS
1	K ₃ SbS ₄ as a Potassium Superionic Conductor with Low Activation Energy for K–S Batteries. Angewandte Chemie - International Edition, 2022, 61, .	7.2	19
2	K ₃ SbS ₄ as a Potassium Superionic Conductor with Low Activation Energy for K–S Batteries. Angewandte Chemie, 2022, 134, .	1.6	4
3	KB ₃ H ₈ ·NH ₃ B ₃ H ₇ Complex as a Potential Solid-State Electrolyte with Excellent Stability against K Metal. ACS Applied Materials & Interfaces, 2022, 14, 17378-17387.	4.0	12
4	Achieving ultralong cycle life graphite binary intercalation in intermediate-concentration ether-based electrolyte for potassium-ion batteries. Carbon, 2022, 196, 229-235.	5.4	8
5	Phase Transferâ€Mediated Degradation of Etherâ€Based Localized Highâ€Concentration Electrolytes in Alkali Metal Batteries. Angewandte Chemie, 2022, 134, .	1.6	4
6	Phase Transferâ€Mediated Degradation of Etherâ€Based Localized Highâ€Concentration Electrolytes in Alkali Metal Batteries. Angewandte Chemie - International Edition, 2022, 61, .	7.2	21
7	K ⁺ Single Cation Ionic Liquids Electrolytes with Low Melting Asymmetric Salt. Journal of Physical Chemistry C, 2022, 126, 11407-11413.	1.5	8
8	Dirhodium(II,II)/NiO Photocathode for Photoelectrocatalytic Hydrogen Evolution with Red Light. Journal of the American Chemical Society, 2021, 143, 1610-1617.	6.6	28
9	Intramolecular Electric Field Construction in Metal Phthalocyanine as Dopantâ€Free Hole Transporting Material for Stable Perovskite Solar Cells with >21 % Efficiency. Angewandte Chemie, 2021, 133, 6364-6369.	1.6	11
10	Intramolecular Electric Field Construction in Metal Phthalocyanine as Dopantâ€Free Hole Transporting Material for Stable Perovskite Solar Cells with >21 % Efficiency. Angewandte Chemie - International Edition, 2021, 60, 6294-6299.	7.2	101
11	Frontispiece: Intramolecular Electric Field Construction in Metal Phthalocyanine as Dopantâ€Free Hole Transporting Material for Stable Perovskite Solar Cells with >21 % Efficiency. Angewandte Chemie - International Edition, 2021, 60, .	7.2	0
12	Single Potassium-Ion Conducting Polymer Electrolytes: Preparation, Ionic Conductivities, and Electrochemical Stability. ACS Applied Energy Materials, 2021, 4, 4156-4164.	2.5	14
13	Frontispiz: Intramolecular Electric Field Construction in Metal Phthalocyanine as Dopantâ€Free Hole Transporting Material for Stable Perovskite Solar Cells with >21 % Efficiency. Angewandte Chemie, 2021, 133, .	1.6	0
14	A Bioinspired Molybdenum Catalyst for Aqueous Perchlorate Reduction. Journal of the American Chemical Society, 2021, 143, 7891-7896.	6.6	26
15	Vibrational Spectroscopy of Beam-Sensitive Materials in the Transmission Electron Microscope. Microscopy and Microanalysis, 2021, 27, 592-594.	0.2	0
16	Antiperovskite K ₃ 0I for K-Ion Solid State Electrolyte. Journal of Physical Chemistry Letters, 2021, 12, 7120-7126.	2.1	33
17	Predictive Design Model for Low-Dimensional Organic–Inorganic Halide Perovskites Assisted by Machine Learning. Journal of the American Chemical Society, 2021, 143, 12766-12776.	6.6	68
18	Alkynyl-Based Covalent Organic Frameworks as High-Performance Anode Materials for Potassium-Ion Batteries. ACS Applied Materials & Interfaces, 2021, 13, 41628-41636.	4.0	37

#	Article	IF	CITATIONS
19	Unusual Melting Trend in an Alkali Asymmetric Sulfonamide Salt Series: Single-Crystal Analysis and Modeling. Inorganic Chemistry, 2021, 60, 14679-14686.	1.9	5
20	Antiperovskite Superionic Conductors: A Critical Review. ACS Materials Au, 2021, 1, 92-106.	2.6	41
21	Grain Boundary Engineering with Self-Assembled Porphyrin Supramolecules for Highly Efficient Large-Area Perovskite Photovoltaics. Journal of the American Chemical Society, 2021, 143, 18989-18996.	6.6	83
22	Forum on Emerging Materials for Catalysis and Energy Applications: In Memory of Professor Chia-Kuang (Frank) Tsung. ACS Applied Materials & Interfaces, 2021, 13, 51807-51808.	4.0	0
23	Unveiling the influence of electrode/electrolyte interface on the capacity fading for typical graphite-based potassium-ion batteries. Energy Storage Materials, 2020, 24, 319-328.	9.5	140
24	A dehydrobenzoannulene-based two-dimensional covalent organic framework as an anode material for lithium-ion batteries. Molecular Systems Design and Engineering, 2020, 5, 97-101.	1.7	37
25	Photoelectrochemical H ₂ O ₂ Production from Oxygen Reduction. ACS Symposium Series, 2020, , 93-109.	0.5	0
26	A Graphite Intercalation Composite as the Anode for the Potassium-Ion Oxygen Battery in a Concentrated Ether-Based Electrolyte. ACS Applied Materials & Interfaces, 2020, 12, 37027-37033.	4.0	9
27	Ambient Pressure X-ray Photoelectron Spectroscopy Investigation of Thermally Stable Halide Perovskite Solar Cells via Post-Treatment. ACS Applied Materials & Interfaces, 2020, 12, 43705-43713.	4.0	34
28	Pursuing graphite-based K-ion O ₂ batteries: a lesson from Li-ion batteries. Energy and Environmental Science, 2020, 13, 3656-3662.	15.6	31
29	Designing Potassium Battery Salts through a Solvent-in-Anion Concept for Concentrated Electrolytes and Mimicking Solvation Structures. Chemistry of Materials, 2020, 32, 10423-10434.	3.2	16
30	Building a Reactive Armor Using S-Doped Graphene for Protecting Potassium Metal Anodes from Oxygen Crossover in K–O ₂ Batteries. ACS Energy Letters, 2020, 5, 1788-1793.	8.8	32
31	Superoxide-Based K–O ₂ Batteries: Highly Reversible Oxygen Redox Solves Challenges in Air Electrodes. Journal of the American Chemical Society, 2020, 142, 11629-11640.	6.6	49
32	From Kâ€O ₂ to Kâ€Air Batteries: Realizing Superoxide Batteries on the Basis of Dry Ambient Air. Angewandte Chemie - International Edition, 2020, 59, 10498-10501.	7.2	33
33	Anthraquinone Redox Relay for Dyeâ€Sensitized Photoâ€electrochemical H ₂ O ₂ Production. Angewandte Chemie - International Edition, 2020, 59, 10904-10908.	7.2	35
34	A reaction-and-assembly approach using monoamine zinc porphyrin for highly stable large-area perovskite solar cells. Science China Chemistry, 2020, 63, 777-784.	4.2	19
35	[Mo2O2S8]2â^' small molecule dimer as a basis for hydrogen evolution reaction (HER) catalyst materials. SN Applied Sciences, 2020, 2, 1.	1.5	8
36	From Kâ€O 2 to Kâ€Air Batteries: Realizing Superoxide Batteries on the Basis of Dry Ambient Air. Angewandte Chemie, 2020, 132, 10584-10587.	1.6	10

#	Article	IF	CITATIONS
37	Anthraquinone Redox Relay for Dyeâ€5ensitized Photoâ€electrochemical H ₂ O ₂ Production. Angewandte Chemie, 2020, 132, 10996-11000.	1.6	7
38	Existence of Ligands within Sol–Gel-Derived ZnO Films and Their Effect on Perovskite Solar Cells. ACS Applied Materials & Interfaces, 2019, 11, 43116-43121.	4.0	28
39	Localized Highâ€Concentration Electrolytes Boost Potassium Storage in Highâ€Loading Graphite. Advanced Energy Materials, 2019, 9, 1902618.	10.2	153
40	Artificial Solidâ€Electrolyte Interphase Enabled Highâ€Capacity and Stable Cycling Potassium Metal Batteries. Advanced Energy Materials, 2019, 9, 1902697.	10.2	81
41	Capillary Encapsulation of Metallic Potassium in Aligned Carbon Nanotubes for Use as Stable Potassium Metal Anodes. Advanced Energy Materials, 2019, 9, 1901427.	10.2	118
42	An Indacenodithieno[3,2â€b]thiopheneâ€Based Organic Dye for Solidâ€State pâ€Type Dyeâ€Sensitized Solar Cel ChemSusChem, 2019, 12, 3243-3248.	lls 3.6	13
43	Excimer-Mediated Intermolecular Charge Transfer in Self-Assembled Donor–Acceptor Dyes on Metal Oxides. Journal of the American Chemical Society, 2019, 141, 8727-8731.	6.6	22
44	Dye-sensitized photocathodes for oxygen reduction: efficient H ₂ O ₂ production and aprotic redox reactions. Chemical Science, 2019, 10, 5519-5527.	3.7	23
45	Anchoring an Artificial Protective Layer To Stabilize Potassium Metal Anode in Rechargeable K–O ₂ Batteries. ACS Applied Materials & Interfaces, 2019, 11, 16571-16577.	4.0	57
46	Decoupling pH Dependence of Flat Band Potential in Aqueous Dye-Sensitized Electrodes. Journal of Physical Chemistry C, 2019, 123, 8681-8687.	1.5	17
47	Monoammonium Porphyrin for Blade-Coating Stable Large-Area Perovskite Solar Cells with >18% Efficiency. Journal of the American Chemical Society, 2019, 141, 6345-6351.	6.6	149
48	Use of Polarization Curves and Impedance Analyses to Optimize the "Triple-Phase Boundary―in K–O2 Batteries. ACS Applied Materials & Interfaces, 2019, 11, 2925-2934.	4.0	10
49	Machine Learning for Understanding Compatibility of Organic–Inorganic Hybrid Perovskites with Post-Treatment Amines. ACS Energy Letters, 2019, 4, 397-404.	8.8	78
50	The Longâ€Term Stability of KO ₂ in Kâ€O ₂ Batteries. Angewandte Chemie - International Edition, 2018, 57, 1227-1231.	7.2	55
51	The Longâ€Term Stability of KO ₂ in Kâ€O ₂ Batteries. Angewandte Chemie, 2018, 130, 1241-1245.	1.6	30
52	Frontispiece: Alkali-Oxygen Batteries Based on Reversible Superoxide Chemistry. Chemistry - A European Journal, 2018, 24, .	1.7	0
53	Chemical Synthesis of K ₂ S ₂ and K ₂ S ₃ for Probing Electrochemical Mechanisms in K–S Batteries. ACS Energy Letters, 2018, 3, 2858-2864.	8.8	64
54	Potassium Superoxide: A Unique Alternative for Metal–Air Batteries. Accounts of Chemical Research, 2018, 51, 2335-2343.	7.6	99

#	Article	IF	CITATIONS
55	Simultaneous Stabilization of Potassium Metal and Superoxide in K–O ₂ Batteries on the Basis of Electrolyte Reactivity. Angewandte Chemie - International Edition, 2018, 57, 10864-10867.	7.2	86
56	Simultaneous Stabilization of Potassium Metal and Superoxide in K–O 2 Batteries on the Basis of Electrolyte Reactivity. Angewandte Chemie, 2018, 130, 11030-11033.	1.6	12
57	Alkaliâ€Oxygen Batteries Based on Reversible Superoxide Chemistry. Chemistry - A European Journal, 2018, 24, 17627-17637.	1.7	13
58	Exploring Stability of Nonaqueous Electrolytes for Potassium-Ion Batteries. ACS Applied Energy Materials, 2018, 1, 1828-1833.	2.5	78
59	Interfacial design of new generation of dye-sensitized photoelectrochemical cells for water oxidation. Science China Chemistry, 2018, 61, 1203-1204.	4.2	7
60	Efficient Grain Boundary Suture by Low-Cost Tetra-ammonium Zinc Phthalocyanine for Stable Perovskite Solar Cells with Expanded Photoresponse. Journal of the American Chemical Society, 2018, 140, 11577-11580.	6.6	95
61	MoS2 as a long-life host material for potassium ion intercalation. Nano Research, 2017, 10, 1313-1321.	5.8	275
62	Preface: Forum on New Materials and Approaches for Beyond Li-ion Batteries. ACS Applied Materials & Interfaces, 2017, 9, 4281-4281.	4.0	2
63	Electrocatalytic Properties of Cuprous Delafossite Oxides for the Alkaline Oxygen Reduction Reaction. ChemCatChem, 2017, 9, 3837-3842.	1.8	10
64	Bilayer Dye Protected Aqueous Photocathodes for Tandem Dye-Sensitized Solar Cells. Journal of Physical Chemistry C, 2017, 121, 8787-8795.	1.5	21
65	Anion-Redox Mechanism of MoO(S ₂) ₂ (2,2′-bipyridine) for Electrocatalytic Hydrogen Production. Journal of the American Chemical Society, 2017, 139, 4342-4345.	6.6	33
66	Electron Transfer Kinetics of a Series of Bilayer Triphenylamine–Oligothiophene–Perylenemonoimide Sensitizers for Dye-Sensitized NiO. Journal of Physical Chemistry C, 2017, 121, 20720-20728.	1.5	13
67	Reversible Dendrite-Free Potassium Plating and Stripping Electrochemistry for Potassium Secondary Batteries. Journal of the American Chemical Society, 2017, 139, 9475-9478.	6.6	395
68	Probing Mechanisms for Inverse Correlation between Rate Performance and Capacity in K–O ₂ Batteries. ACS Applied Materials & Interfaces, 2017, 9, 4301-4308.	4.0	49
69	Greatly Enhanced Anode Stability in Kâ€Oxygen Batteries with an In Situ Formed Solvent―and Oxygenâ€Impermeable Protection Layer. Advanced Energy Materials, 2017, 7, .	10.2	34
70	Tunable Molecular MoS ₂ Edge-Site Mimics for Catalytic Hydrogen Production. Inorganic Chemistry, 2016, 55, 3960-3966.	1.9	53
71	[MoO(S ₂) ₂ L] ^{1–} (L = picolinate or pyrimidine-2-carboxylate) Complexes as MoS _{<i>x</i>} -Inspired Electrocatalysts for Hydrogen Production in Aqueous Solution. Journal of the American Chemical Society, 2016, 138, 13726-13731.	6.6	41
72	pH-Tuning a Solar Redox Flow Battery for Integrated Energy Conversion and Storage. ACS Energy Letters, 2016, 1, 578-582.	8.8	55

Yiying Wu

#	Article	IF	CITATIONS
73	Concentrated Electrolyte for the Sodium–Oxygen Battery: Solvation Structure and Improved Cycle Life. Angewandte Chemie, 2016, 128, 15536-15540.	1.6	20
74	Concentrated Electrolyte for the Sodium–Oxygen Battery: Solvation Structure and Improved Cycle Life. Angewandte Chemie - International Edition, 2016, 55, 15310-15314.	7.2	97
75	Exploring Thermal Properties of M0S2 Using In Situ Quantitative STEM. Microscopy and Microanalysis, 2016, 22, 912-913.	0.2	0
76	Solar-powered electrochemical energy storage: an alternative to solar fuels. Journal of Materials Chemistry A, 2016, 4, 2766-2782.	5.2	109
77	Membrane-Inspired Acidically Stable Dye-Sensitized Photocathode for Solar Fuel Production. Journal of the American Chemical Society, 2016, 138, 1174-1179.	6.6	122
78	Dimeric [Mo ₂ S ₁₂] ^{2â^'} Cluster: A Molecular Analogue of MoS ₂ Edges for Superior Hydrogenâ€Evolution Electrocatalysis. Angewandte Chemie - International Edition, 2015, 54, 15181-15185.	7.2	160
79	Dye ontrolled Interfacial Electron Transfer for High urrent Indium Tin Oxide Photocathodes. Angewandte Chemie - International Edition, 2015, 54, 6857-6861.	7.2	35
80	2H-CuScO ₂ Prepared by Low-Temperature Hydrothermal Methods and Post-Annealing Effects on Optical and Photoelectrochemical Properties. Inorganic Chemistry, 2015, 54, 5519-5526.	1.9	27
81	Investigating dendrites and side reactions in sodium–oxygen batteries for improved cycle lives. Chemical Communications, 2015, 51, 7665-7668.	2.2	93
82	Potassium-Ion Oxygen Battery Based on a High Capacity Antimony Anode. ACS Applied Materials & Interfaces, 2015, 7, 26158-26166.	4.0	227
83	p-type doping of MoS ₂ thin films using Nb. Applied Physics Letters, 2014, 104, 092104.	1.5	268
84	Electron transport in large-area epitaxial MoS2. , 2014, , .		1
85	Cu(i)-based delafossite compounds as photocathodes in p-type dye-sensitized solar cells. Physical Chemistry Chemical Physics, 2014, 16, 5026.	1.3	116
86	A double-acceptor as a superior organic dye design for p-type DSSCs: high photocurrents and the observed light soaking effect. Physical Chemistry Chemical Physics, 2014, 16, 26103-26111.	1.3	55
87	Understanding Side Reactions in K–O ₂ Batteries for Improved Cycle Life. ACS Applied Materials & Interfaces, 2014, 6, 19299-19307.	4.0	117
88	Integrating a redox-coupled dye-sensitized photoelectrode into a lithium–oxygen battery for photoassisted charging. Nature Communications, 2014, 5, 5111.	5.8	236
89	Scalable synthesis of delafossite CuAlO2 nanoparticles for p-type dye-sensitized solar cells applications. Journal of Alloys and Compounds, 2014, 591, 275-279.	2.8	74
90	Understanding the Crystallization Mechanism of Delafossite CuGaO ₂ for Controlled Hydrothermal Synthesis of Nanoparticles and Nanoplates. Inorganic Chemistry, 2014, 53, 5845-5851.	1.9	70

Yiying Wu

#	Article	lF	CITATIONS
91	Molecular Orbital Engineering of a Panchromatic Cyclometalated Ru(II) Dye for p-Type Dye-Sensitized Solar Cells. Journal of Physical Chemistry C, 2014, 118, 16518-16525.	1.5	34
92	Photostable p-Type Dye-Sensitized Photoelectrochemical Cells for Water Reduction. Journal of the American Chemical Society, 2013, 135, 11696-11699.	6.6	189
93	Photoinduced Electron Transfer Dynamics of Cyclometalated Ruthenium (II)–Naphthalenediimide Dyad at NiO Photocathode. Journal of Physical Chemistry C, 2013, 117, 18315-18324.	1.5	44
94	Low frequency noise in chemical vapor deposited MoS <inf>2</inf> . , 2013, , .		4
95	A Low-Overpotential Potassium–Oxygen Battery Based on Potassium Superoxide. Journal of the American Chemical Society, 2013, 135, 2923-2926.	6.6	298
96	Large area single crystal (0001) oriented MoS2. Applied Physics Letters, 2013, 102, .	1.5	200
97	Cyclometalated Ruthenium Sensitizers Bearing a Triphenylamino Group for p-Type NiO Dye-Sensitized Solar Cells. ACS Applied Materials & Interfaces, 2013, 5, 8641-8648.	4.0	68
98	Probing the Low Fill Factor of NiO p-Type Dye-Sensitized Solar Cells. Journal of Physical Chemistry C, 2012, 116, 26239-26246.	1.5	94
99	The Effect of an Atomically Deposited Layer of Alumina on NiO in P-type Dye-Sensitized Solar Cells. Langmuir, 2012, 28, 950-956.	1.6	66
100	Synthesis, Photophysics, and Photovoltaic Studies of Ruthenium Cyclometalated Complexes as Sensitizers for p-Type NiO Dye-Sensitized Solar Cells. Journal of Physical Chemistry C, 2012, 116, 16854-16863.	1.5	81
101	Valence Band-Edge Engineering of Nickel Oxide Nanoparticles via Cobalt Doping for Application in p-Type Dye-Sensitized Solar Cells. ACS Applied Materials & Interfaces, 2012, 4, 5922-5929.	4.0	119
102	p-Type Dye-Sensitized Solar Cells Based on Delafossite CuGaO ₂ Nanoplates with Saturation Photovoltages Exceeding 460 mV. Journal of Physical Chemistry Letters, 2012, 3, 1074-1078.	2.1	154
103	Sonochemical synthesis of copper hydride (CuH). Chemical Communications, 2012, 48, 1302-1304.	2.2	32
104	Linker effect in organic donor–acceptor dyes for p-type NiO dye sensitized solar cells. Energy and Environmental Science, 2011, 4, 2818.	15.6	110
105	NANOCRYSTALLINE OXIDE SEMICONDUCTORS FOR DYE-SENSITIZED SOLAR CELLS. , 2011, , 127-173.		0
106	p-Type Dye-Sensitized NiO Solar Cells: A Study by Electrochemical Impedance Spectroscopy. Journal of Physical Chemistry C, 2011, 115, 25109-25114.	1.5	101
107	Preparation, characterization, and electrocatalytic performance of graphene-methylene blue thin films. Nano Research, 2011, 4, 124-130.	5.8	35
108	Ni _{<i>x</i>} Co _{3â^'<i>x</i>} O ₄ Nanowire Arrays for Electrocatalytic Oxygen Evolution. Advanced Materials, 2010, 22, 1926-1929.	11.1	837

#	Article	IF	CITATIONS
109	Electrocatalytic Activity of Graphene Multilayers toward Iâ^'/I3â^': Effect of Preparation Conditions and Polyelectrolyte Modification. Journal of Physical Chemistry C, 2010, 114, 15857-15861.	1.5	63
110	Photoelectrochemical Study of the Ilmenite Polymorph of CdSnO ₃ and Its Photoanodic Application in Dye-Sensitized Solar Cells. Journal of Physical Chemistry C, 2010, 114, 6802-6807.	1.5	42
111	Critical Role of Screw Dislocation in the Growth of Co(OH) ₂ Nanowires as Intermediates for Co ₃ O ₄ Nanowire Growth. Chemistry of Materials, 2010, 22, 5537-5542.	3.2	56
112	Formation of Na0.44MnO2 nanowires via stress-induced splitting of birnessite nanosheets. Nano Research, 2009, 2, 54-60.	5.8	53
113	Mesoporous Nb-Doped TiO ₂ as Pt Support for Counter Electrode in Dye-Sensitized Solar Cells. Journal of Physical Chemistry C, 2009, 113, 7456-7460.	1.5	59
114	Photoelectrochemical Study of the Band Structure of Zn ₂ SnO ₄ Prepared by the Hydrothermal Method. Journal of the American Chemical Society, 2009, 131, 3216-3224.	6.6	246
115	Nanoscale design to enable the revolution in renewable energy. Energy and Environmental Science, 2009, 2, 559.	15.6	348
116	Ammonia-Evaporation-Induced Synthetic Method for Metal (Cu, Zn, Cd, Ni) Hydroxide/Oxide Nanostructures. Chemistry of Materials, 2008, 20, 567-576.	3.2	142
117	Mesoporous Co ₃ O ₄ Nanowire Arrays for Lithium Ion Batteries with High Capacity and Rate Capability. Nano Letters, 2008, 8, 265-270.	4.5	1,234
118	Zinc Stannate (Zn2SnO4) Dye-Sensitized Solar Cells. Journal of the American Chemical Society, 2007, 129, 4162-4163.	6.6	379
119	Assembly of spherical micelles in 2D physical confinements and their replication into mesoporous silica nanorods. Journal of Materials Chemistry, 2007, 17, 4558.	6.7	24
120	Dye-Sensitized Solar Cells Based on Anatase TiO2Nanoparticle/Nanowire Composites. Journal of Physical Chemistry B, 2006, 110, 15932-15938.	1.2	578
121	Characterization of heat transfer along a silicon nanowire using thermoreflectance technique. IEEE Nanotechnology Magazine, 2006, 5, 67-74.	1.1	36
122	Engineering Nanostructures for Single-Molecule Surface-Enhanced Raman Spectroscopy. Israel Journal of Chemistry, 2006, 46, 283-291.	1.0	1
123	Freestanding Mesoporous Quasi-Single-Crystalline Co3O4Nanowire Arrays. Journal of the American Chemical Society, 2006, 128, 14258-14259.	6.6	338
124	Engineering Nanostructures for Single-Molecule Surface-Enhanced Raman Spectroscopy. Israel Journal of Chemistry, 2006, 46, 283-291.	1.0	0
125	Single-Crystal Mesoporous Silica Ribbons. Angewandte Chemie - International Edition, 2005, 44, 332-336.	7.2	50
126	Composite mesostructures by nano-confinement. Nature Materials, 2004, 3, 816-822.	13.3	626

#	Article	IF	CITATIONS
127	Templated Synthesis of Highly Ordered Mesostructured Nanowires and Nanowire Arrays. Nano Letters, 2004, 4, 2337-2342.	4.5	205
128	Synthesis and photocatalytic properties of highly crystalline and ordered mesoporous TiO2 thin films. Chemical Communications, 2004, , 1670.	2.2	142
129	Thermal conductivity of Si/SiGe superlattice nanowires. Applied Physics Letters, 2003, 83, 3186-3188.	1.5	355
130	Thermal conductivity of individual silicon nanowires. Applied Physics Letters, 2003, 83, 2934-2936.	1.5	1,536
131	Fabrication of Silica Nanotube Arrays from Vertical Silicon Nanowire Templates. Journal of the American Chemical Society, 2003, 125, 5254-5255.	6.6	257
132	INORGANIC SEMICONDUCTOR NANOWIRES. International Journal of Nanoscience, 2002, 01, 1-39.	0.4	155
133	Block-by-Block Growth of Single-Crystalline Si/SiGe Superlattice Nanowires. Nano Letters, 2002, 2, 83-86.	4.5	942
134	Inorganic Semiconductor Nanowires: Rational Growth, Assembly, and Novel Properties. Chemistry - A European Journal, 2002, 8, 1260-1268.	1.7	394
135	Room-Temperature Ultraviolet Nanowire Nanolasers. Science, 2001, 292, 1897-1899.	6.0	8,567
136	Direct Observation of Vaporâ^'Liquidâ^'Solid Nanowire Growth. Journal of the American Chemical Society, 2001, 123, 3165-3166.	6.6	980
137	Metal Nanowire Formation Using Mo3Se3-as Reducing and Sacrificing Templates. Journal of the American Chemical Society, 2001, 123, 10397-10398.	6.6	89
138	Germanium/carbon core–sheath nanostructures. Applied Physics Letters, 2000, 77, 43-45.	1.5	84
139	Germanium Nanowire Growth via Simple Vapor Transport. Chemistry of Materials, 2000, 12, 605-607.	3.2	448
140	Measurements of Bi/sub 2/Te/sub 3/ nanowire thermal conductivity and Seebeck coefficient. , 0, , .		7